Cellulose
https://doi.org/10.1007/s10570-022-04522-9

ORIGINAL RESEARCH

Characterization, optimization, and evaluation of preservative efficacy of carboxymethyl cellulose/hydromagnesite stromatolite bio-nanocomposite

Selcan Karakuş · Mert Akın Insel · İbrahim Mizan Kahyaoğlu · İnci Albayrak · Fulya Ustun-Alkan

Received: 1 October 2021 / Accepted: 2 March 2022

Abstract Currently, researchers are focusing on the development of nano-additive preservatives during the worldwide COVID-19 pandemic. This research aimed to constitute a small sized preservative nano-formulation which emerges from the biopolymer carboxymethyl cellulose (a green stabilizing agent) and hydromagnesite stromatolite (a fossilized natural additive). In this study, we investigated the optimization of the experimental design of carboxymethyl cellulose/hydromagnesite stromatolite (CMC/HS) bio-nanocomposites using a green and one-step sonochemical method at room temperature. In addition, we constructed a mathematical model which relates the intrinsic viscosity with all operating variables, and we carried out statistical error analysis to assess the validity of the proposed model. The characterization and chemical functional groups of CMC/HS bio-nanocomposites were determined by different advanced techniques such as SEM, HRTEM, DLS, FTIR, XRD, and BET. The challenge test was used to show the preservative efficacy of CMC/HS bio-nanocomposites against Staphylococcus aureus, Pseudomonas aeruginosa, Escherichia coli, Candida albicans, and Aspergillus brasiliensis. The 3-(4,5-dimethylthiazol-2-yl)-2,5-diphenyltrazolium bromide (MTT) assay was performed on L929 cells to evaluate the in vitro cytotoxicity of CMC/HS bio-nanocomposites. According to the results, we showed that the synthesized CMC/HS bio-nanocomposites have no cytototoxic effects on L929 fibroblast cells and could be considered to be an alternative green nano-additive preservative against pathogenic microorganisms.

Keywords Nano-additive · Carboxymethyl cellulose · Biopolymer

S. Karakuş (✉)
Department of Chemistry, Faculty of Engineering, Istanbul University-Cerrahpasa, 34320 Avcilar, Istanbul, Turkey
e-mail: selcan@iuc.edu.tr

M. A. Insel
Department of Chemical Engineering, Yıldız Technical University, 34210 Istanbul, Turkey

İ. M. Kahyaoğlu
Department of Chemistry, Ondokuz Mayis University, 55139 Kurupelit, Samsun, Turkey

İ. Albayrak
Department of Mathematical Engineering, Yıldız Technical University, Istanbul 34210, Turkey

F. Ustun-Alkan
Faculty of Veterinary Medicine, Department of Pharmacology and Toxicology, Istanbul University-Cerrahpasa, 34500 Istanbul, Turkey

Introduction

Recent advances in nanotechnological studies aim to protect against pathogenic microorganisms, prevent emerging infectious diseases, and detect multiple pathogenic bacteria (Baptista et al. 2018; Ahmed

Published online: 22 March 2022

et al. 2020; Alafeef et al. 2020; Ghosh et al. 2021). Antimicrobial, antifungal, and antiviral nanostructures are attractive alternatives due to their biocompatibility and bio-degradability, and their preservative properties in food packaging, textiles, cosmetics, and biomedical applications (Sharma et al. 2020; Barman et al. 2020; Shahvalizadeh et al. 2021; Guo et al. 2021). Over the past two decades, cosmetic preservatives such as bio-nanocomposites have received great interest against pathogenic microorganisms such as bacteria, fungi, parasites, and viruses (Connolly et al. 2019; Saadat et al. 2020). Advanced bio-nanocomposites have remarkable physiochemical, biological, mechanical, thermo-physical, microstructural, and barrier properties, and they provide a significant potential for safe preservatives and a new generation of broad-spectrum antimicrobial and antifungal nano-agents (Wang et al. 2021; Awad et al. 2021; Kouser et al. 2021). Furthermore, the enhancement of unique morphology and chemical properties of the green bio-nanocomposites has been reported, as well as their biodegradability, antimicrobial properties, and mechanical and thermal properties for food packaging and cosmetic applications (Scaffaro et al. 2017; Murali et al. 2019). Bio-nanocomposites have significant biological activity due to their uniform size distribution, homogeneous dispersion, and nanoscale sizes, ranging from 1 to 1000 nm in diameter (Nguyen et al. 2021; Sahoo et al. 2021). According to scientific trends, several previous studies have highlighted the antimicrobial mechanism of action of synthesized green and low-cost bio-nanocomposites (Othman et al. 2021; Moghadam et al. 2021; Kumaravel et al. 2021; Shahvalizadeh et al. 2021). Nguyen et al. investigated the antimicrobial activity of chitosan/ZnO bio-nanocomposites prepared via a green process using orange peel extract as a reducing agent (Nguyen et al. 2021). Abduraimova et al. showed that a synthesized cetyltrimethylammonium bromide (CTAB)-loaded SiO_2–silver mesoporous nanocomposite was an efficient antibacterial agent which exhibited antimicrobial properties against Gram-negative and Gram-positive bacterial strains (Abduraimova et al. 2021). Hassanen et al. examined the in vivo and in vitro antibacterial potential of chitosan-silver nanocomposites against methicillin-resistant Staphylococcus aureus (S. aureus) induced infection in rats (Hassanen and Ragab 2020). Yunusov et al. showed that synthesized carboxymethylcellulose and silver nanoparticles had a high antimicrobial activity against *Staphylococcus epidermidis* (*S. epidermidis*) and the yeast fungus *Candida albicans* (*C. albicans)* (Yunusov et al. 2021). Wang et al. synthesized MgO/carboxymethyl chitosan nanocomposites to improve their thermal stability, water resistance, and antibacterial performance. The antibacterial activities of the synthesized nanostructures against food-related microorganisms such as Listeria monocytogenes and Shewanella baltica were reported (Wang et al. 2020). Rao et al. investigated the hemostatic, biocompatible, and antibacterial non-animal fungal mushroom-based carboxymethyl chitosan-ZnO nanocomposite for wound-healing applications. The results showed that bio-nanocomposites had a spherical shape and an average diameter of 18 ± 3.6 nm with synergetic antibacterial properties against Gram-positive (*Staphylococcus aureus*) bacteria and good hemocompatibility (Rao et al. 2020). Jannatyha et. al compared the mechanical, barrier, and antimicrobial properties of synthesized nanocellulose/CMC and nanochitosan/CMC composite films. They showed that the CMC nanocomposite films had potential for application in food packaging (Jannatyha et al. 2020). To the best of our knowledge, there are no previous reports on the preparation of CMC/hydromagnesite stromatolite bio-nanocomposite via a green sonication method. In addition, this study highlighted the first report of the evaluation of the preservative efficacy of CMC/hydromagnesite stromatolite bio-nanocomposite.

Carboxymethyl cellulose (CMC) is a water-soluble, non-toxic, and low-cost polysaccharide. It consists of D-glucose residues linked by β-1,4-linkage, and it is used as a green stabilizing/capping agent (Kasirajan and Maupin-Furlow 2021). Natural hydromagnesite stromatolites are formed by microbially induced precipitation of hydromagnesite (Braithwaite and Zedef 1994).

Due to their high resistance, nanostructure based antimicrobial agents are promising antibacterial agents as biologically active additives (Zhang et al. 2016; Navik et al. 2017; Amina et al. 2021). In the literature, we noticed that Na-CMC with 250 kDa molecular weight based microparticles as storage vehicles were used for plant extract (Tsirigotis-Maniecka 2020). Na-CMC is a biocompatible and biodegradable polymer. With this approach, the polymer matrix CMC was chosen for applications in edible coatings and cosmetics. This study was aimed to prepare a novel preservative

nano-formulation which was obtained from carboxymethyl cellulose biopolymer (as a green stabilizing agent) and hydromagnesite stromatolite (as a fossilized natural additive). In this study, we preferred HS as a green additive. These hydrated Mg-rich stromatolites have an environmentally friendly nature for antimicrobial applications. The novel carboxymethyl cellulose/hydromagnesite stromatolite (CMC/HS) bio-nanocomposites were prepared using a green and one-step sonochemical method at room temperature. The characterization and chemical functional groups of CMC/HS bio-nanocomposites were determined using different techniques such as scanning electron microscopy (SEM), high resolution transmission electron microscopy (HRTEM), Fourier transform infrared (FTIR) spectroscopy, X-ray diffraction (XRD), dynamic light scattering (DLS), and the Brunauer–Emmett–Teller (BET) technique. Furthermore, the aim of this study was focused on the fabrication and optimization of the synthesized CMC/HS bio-nanocomposites to obtain a novel preservative nanomaterial for antimicrobial and antifungal agents in biomedical applications. We investigated the effects of the operating variables (temperature (T = 25–45 °C), sonication time (t_s = 10–60 min), concentration (C = 75–450 g/ml), and mass ratio of CMC/HS (MR = 2:1–4:1)) on the intrinsic viscosity. A mathematical model was constructed which represents the relationship between the intrinsic viscosity and all the operating variables. Error analysis was conducted to evaluate the validity of the constructed model. As a result, it was shown that the constructed model sufficiently represents the data. The proposed model may also be utilized to obtain intrinsic viscosity within the specified interval for operating variables without conducting any experiments. Finally, we proved the preservative efficacy of the synthesized CMC/HS bio-nanocomposites against microorganisms such as *Candida albicans (C. albicans), Escherichia coli (E. coli), Pseudomonas aeruginosa (P. aeruginosa), Aspergillus brasiliensis (A. brasiliensis),* and *Staphylococcus aureus (S. aureus)* using the ISO 11930:2012 guideline.

Materials and methods

Materials

Carboxymethyl cellulose (CMC) (molecular weight: 250 kDa, the degree of substitution: 0.90, 2% in water at 25 °C) and TWEEN® 20 (for molecular biology, viscous liquid) were purchased from Sigma-Aldrich Company (USA). HS was collected from Salda Lake, Yeşilova (Burdur) in Turkey. A sterile syringe filter with a polyvinylidene difluoride (PVDF) membrane (0.22-micron) was preferred for sterilizing non-sterile samples. All chemicals and reagents were used without further purification.

The preparation of CMC/HS bio-nanocomposites

The preparation process of CMC/HS bio-nanocomposites had four steps. In the first step, 0.1 g of CMC was dissolved in 100 ml of distilled water at 25 °C. In the second step, 0.05 g of HS was added to CMC solution and stirred for 10 min at 25 °C. In the third step, 1 ml of Tween 20 added to the sample. Finally, the solution was sonicated for 60 min at amplitude frequency 30% at 45 °C and filtered using a sterile syringe filter.

Characterization of CMC/HS bio-nanocomposites

The characterization and identification of the chemical functional groups of CMC/HS bio-nanocomposites were determined by different techniques such as scanning electron microscopy (SEM, FEI QUANTA 450) with a double-coated, 8 mmW × 20 ml, high resolution transmission electron microscopy (HRTEM) (Hitachi, HighTech HT7700) in a high vacuum mode at 100 kV, Fourier transform infrared (FTIR) (Perkin Elmer Spectrum Two) spectroscopy in the 4000–400 cm^{-1} frequency range with a resolution of 4 cm^{-1} and 8 scans, X-ray diffraction (XRD) with Cu Kα radiation at 40 kV and 15 mA, dynamic light scattering (DLS, Dawn Heleos II Wyatt) at 658 wavelength and a scattering angle of 90°, and Brunauer–Emmett–Teller (BET, Micromeritics ASAP 2020) techniques.

Calculations and Experimental Optimizations

The crystalline size of CMC/HS bio-nanocomposites was calculated using the Scherrer formula. The formula of the Scherrer model is given in Eq. 1 (Kibasomba et al. 2018).

$$D_p = \frac{0.94.\lambda}{\beta.\cos\theta} \quad (1)$$

where D_p is the average crystallite size, β is line broadening in radians, θ is the Bragg angle, and λ is the X-Ray wavelength.

In this study, we investigated the optimization of the experimental operating parameters for the preparation of CMC/HS bio-nanocomposites using a simple dilute solution methodology with different experimental media. For this reason, we examined the rheological behavior of CMC/HS bio-nanocomposites to determine the effects of CMC/HS (4:1, 3:1, and 2:1), sonication time (10–60 min), and temperature (25–45 °C) on the synthesis of the CMC/HS bio-nanocomposites. In Tables 1 and 2, different experimental operating parameters are presented for the design in the preparation of CMC/HS bio-nanocomposites.

The intrinsic viscosity of the synthesized CMC/HS bio-nanocomposites was investigated to optimize the nanostructure in a dilute solution at different operating parameters such as mixing ratios, temperatures, and sonication times. For this purpose, the intrinsic viscosity of CMC/HS bio-nanocomposites was measured using a viscometer with the WinCT-Viscosity software. The specific viscosity (η_{sp}) and the intrinsic viscosity ([η]) were calculated using Eqs. 2 and 3, respectively (Nishida et al. 2002):

$$\eta_{sp} = \frac{t}{t_0} - 1 \quad (2)$$

$$[\eta] = \lim_{C \to 0} \left(\frac{\eta_{sp}}{C} \right) \quad (3)$$

We calculated the parameters of the multi-concentration regression model (Huggins model) using Eq. 2.5 (Karakus et al. 2019).

$$\eta_{sp}/C = [\eta] + k_1[\eta]^2 C \quad (4)$$

k_1: Huggins constant and C: concentration.

Pathogen challenge test

In this study, the synthesized CMC/HS bio-nanocomposites were tested against different pathogenic microorganisms such as *S. aureus* (NCTC 10788), *P. aeruginosa* (ATCC 9027), *E. coli* (ATCC 8739), *C. albicans* (NCPF 3179), and *A. brasiliensis* (NCPF 2275) using the standard NF EN ISO 11930:2012 method (Table 3). We examined the synthesized CMC/HS bio-nanocomposites by inoculation with

Table 1 Different experimental operating parameters for the design in the preparation of CMC/HS bio-nanocomposites

Run	Sample	Experimental parameters		
		Sonication time (min)	Mass ratio of CMC/HS	Temperature (°C)
1	CMC/HS bio-nanocomposites (4:1)	10	4:1	25
2		30	4:1	25
3		60	4:1	25
4		60	4:1	35
5		60	4:1	45
6	CMC/HS bio-nanocomposites (3:1)	10	3:1	25
7		30	3:1	25
8		60	3:1	25
9		60	3:1	35
10		60	3:1	45
11	CMC/HS bio-nanocomposites (2:1)	10	2:1	25
12		30	2:1	25
13		60	2:1	25
14		60	2:1	35
15		60	2:1	45

Table 2 The design methodology for the CMC/HS bio-nanocomposites

Run	Sample	Factors		
		Sonication time	Mass ratio	Temperature
		Levels	Levels	Levels
1	CMC/HS bio-nanocomposites (4:1)	−1	+1	−1
2		0	+1	−1
3		+1	+1	−1
4		+1	+1	0
5		+1	+1	+1
6	CMC/HS bio-nanocomposites (3:1)	−1	0	−1
7		0	0	−1
8		+1	0	−1
9		+1	0	0
10		+1	0	+1
11	CMC/HS bio-nanocomposites (2:1)	−1	+1	−1
12		0	+1	−1
13		+1	+1	−1
14		+1	+1	0
15		+1	+1	+1

+1: maximum experimental parameter and − 1: minimum parameter for the experimental factors

different microorganisms at concentrations ranging from 10^5 to10^6 CFU g^{-1} corresponding to the colony forming units per g of the synthesized CMC/HS bio-nanocomposites.

The challenge tests were performed against all pathogenic microorganisms, which were issued from official collection of microbial strains of The European Union (EU). This ensures the reproducibility of the test. Also, the inoculated CMC/HS bio-nanocomposites were held at temperatures ranging from 20 to 25 °C in the dark room for twenty-eight days. The viability assessment was performed at suitable time intervals:

T_0: zero storage days, immediately after collection,
T_7: seven storage days,
T_{14}: fourteen storage days,
T_{28}: twenty-eight storage days with the number of viable pathogenic microorganisms. The challenge test was determined with criteria A and B, which were presented in Table 4.

Criteria A and B of challenge test were defined from decreases of logarithmic reduction scale 10 of pathogenic microorganism concentration from the measured inoculum using the standard NF EN ISO 11930 process for the evaluation the biological properties such as the antimicrobial and antifungal properties of the prepared nano-formulas. The results of challenge tests were presented at different levels such as A (a target level) and B (an acceptable level). According to experimental results, “no increase” was

Table 3 The challenge test process for the synthesized CMC/HS bio-nanocomposites

Microorganisms		Method	
		Medium	Temperature (°C)
S. aureus	NCTC 10788/Lot 0350520029	Tryptic Soy Agar	30–35
P. aeruginosa	ATCC 9027/Lot 3270513	Tryptic Soy Agar	30–35
E. coli	ATCC 8739/Lot 4835151	Tryptic Soy Agar	30–35
C. albicans	NCPF 3179/Lot 040920020	Saboraud 4% Dextrose Agar	20–25
A. brasiliensis	NCPF 2275/Lot 020620065	Saboraud 4% Dextrose Agar	20–25

Table 4 The criteria for the preservative effectiveness test of the synthesized CMC/HS bio-nanocomposites

Microorganism	*S. aureus, P. aeruginosa,* and *E. coli*			*C. albicans*			*A. brasiliensis*	
Time	*T7*	*T14*	*T28*	*T7*	*T14*	*T28*	*T14*	*T28*
Criteria A	≧3	≧3 log	≧3 log	≧1	≧3 log	≧1 log	≧0	≧1
Criteria B	Not performed	≧3	≧3 log	Not performed	≧1	≧1 log	≧0	≧9 log

defined as not much more than 0.5 log10 units higher than the previous value measured.

In vitro cytotoxicity analysis

The cytotoxic effect was measured using the MTT (3-(4,5-dimethylthiazol-2-yl)-2,5-diphenyltrazolium bromide) assay. For this purpose, L929 cells (mouse fibroblast cell line) were cultured in high glucose Dulbecco's Modified Eagle's Medium (Sigma-Aldrich) supplemented with 10% fetal bovine serum and 100 IU/ml Penicillin–100 µg/ml Streptomycin (Gibco) in a humidified atmosphere containing 5% CO_2 at 37 °C. Briefly, L929 cells were seeded in 96-well plates at a density of 1×10^4 cells/well in medium and incubated at 37 °C in a humidified atmosphere of 5% CO_2 for 24 h. Then, the medium was removed, and the cells were treated with varying concentrations of CMC, HS, and CMC/HS bio-nanocomposites (10 µg/ml, 50 µg/ml, and 100 µg/ml) for 24 h. At the end of the treatment, 10 µl of MTT solution (0.5 mg/ml) was added to each well. After 4 h of incubation, 100 µl DMSO was added to each well for the solubilization of MTT formazan crystals. Following 10 min incubation in dark, the absorbance of the wells was measured at a wavelength of 595 nm using a microplate reader (FilterMax F5, Molecular Devices, USA). All samples were tested in triplicate, and the mean for each experiment was calculated. The effect of CMC/HS bio-nanocomposites on cell viability was assessed as percent cell viability, where untreated cells which served as a control were considered 100% viable. All samples were tested in triplicate, and the mean for each experiment was calculated.

Statistical analysis of experimental results

All experimental results were obtained in triplicate and are given as the mean for each experiment. The analysis of variance (ANOVA) procedure was conducted in SPSS (version 16, Chicago) with a significance level of $p<0.05$.

Mathematical modelling of intrinsic viscosity

To obtain a mathematical model which relates operating variables with the intrinsic viscosity, two polynomial surfaces were fitted to the data of CMC/HS weight ratio – concentration – intrinsic viscosity (F1) and sonication time – concentration – intrinsic viscosity (F2). A linear regression was applied to obtain the relationship between temperature and intrinsic viscosity (F3). Then, the latter surface (F2) and the line (F3) were normalized with respect to fixed parameters, T = 25 °C and $t_s = 60$ min. Finally, the former surface (F1) is multiplied by normalized functions (F2 and F3). Consequently, the function is obtained whose inputs are all operating variables and the output is intrinsic viscosity.

Statistical error analysis

Statistical error analysis was conducted to assess the validity of the constructed model. The sum of squares of errors (SSE), the hybrid fractional error function (HYBRID), Marquart's percentage standard deviation (MPSD), and the average relative error (ARE) were computed by using Eqs. 5–8 (Karakuş et al. 2021). The correlation diagram is also presented to clarify the validity of the model.

$$SSE = \sum_{i=1}^{n} \left([\eta]_{cal} - [\eta]_e\right)_i^2 \tag{5}$$

$$HYBRID = \frac{100}{n-p} \sum_{i=1}^{n} \left[\frac{\left([\eta]_e - [\eta]_{cal}\right)_i^2}{\gamma_e} \right] \tag{6}$$

$$MPSD = 100\sqrt{\frac{1}{n-p}\sum_{i=1}^{n}\left(\frac{[\eta]_e - [\eta]_{cal}}{[\eta]_e}\right)_i^2} \quad (7)$$

$$ARE = \frac{100}{n-p}\sum_{i=1}^{n}\left|\frac{[\eta]_e - [\eta]_{cal}}{[\eta]_e}\right|_i \quad (8)$$

Here, $[\eta]_e$ is experimental intrinsic viscosity, $[\eta]_{cal}$ is the calculated intrinsic viscosity, n is the number of data points, and p is the number of parameters.

Results and discussion

Characterization of CMC/HS bio-nanocomposites

In this study, HS was used as a stabilizing agent for the novel bio-nanocomposite. According to characterization results, we aimed to calculate the crystalline size, dispersion, and shape of the CMC/HS bio-nanocomposites. The SEM and HRTEM techniques were used to determine the surface, particle size, and hydrodynamic diameter of the CMC/HS bio-nanocomposites. SEM micrographs of HS and CMC/HS bio-nanocomposites are given in Fig. 1a, b. Also, HRTEM images of CMC/HS bio-nanocomposites and DLS hydrodynamic diameter distribution histograms of CMC/HS bio-nanocomposites are given in Fig. 1c, d. The SEM result showed that HS had 3D irregularly shaped particles with a heterogeneous porous surface (Fig. 1a) (Karakuş et al. 2020).

SEM and HRTEM images (Fig. 1b, c) of CMC/HS bio-nanocomposites showed that the nanostructure had a uniform two-dimensional (2D) morphology and exfoliated nanosheets within biopolymer network at nanoscale. Surface characterization results revealed the dissociated 2D layers of the synthesized CMC/HS bio-nanocomposites. To our knowledge, this is the first report of the preparation and characterization of fossilized natural additive based bio-nanocomposites. Our data indicated that the surface morphologies of fossilized based bio-nanocomposites have a homogeneous 2D nanostructure, a result that casts a new light on the preparation of fossilized based nanostructures via a green sonication process. The DLS hydrodynamic diameter distribution histogram of CMC/HS bio-nanocomposites is presented in Fig. 1d. The DLS laser particle analyzer result of CMC/HS bio-nanocomposites showed that the particle size of the CMC/HS bio-nanocomposites dispersed in deionized water was ~98 nm. The polydispersity index (PDI) was calculated from the standard deviation (σ) of the particle diameter distribution divided by the mean particle diameter using the DLS technique for the nanostructure. The PDI of CMC/HS bio-nanocomposites the was found to be ~ 0.160. Also, according to BET results, we found that the surface area was 180.66 m^2/g.

X-ray Diffraction (XRD) results of (a) HS and (b) CMC/HS bio-nanocomposites are given in Fig. 2 and performed to calculate the crystalline size of HS characteristic peaks. The measurement was conducted between 2θ values of 2° and 70°. XRD results showed that characteristic peaks of HS were observed at 2θ = 9.5°, 12.0°, 13.7°, 15.2°, 19.8°, 21.2°, and 30.8° corresponded to the mineral Hydromagnesite crystal structure with a PDF-4 + 2022 code: 04-013-7631 ((Å):10.1050, b (Å):8.9540, and c (Å): 8.3780) (Akao et al. 1977). The crystal system of the HS was monoclinic, space group was P21/c, and space group number was 14. Intrestingly, the peak at 12.0° was unanticipated since the P21/c space group predicts that a peak at 11.8° would be missing, thus, the occurance of this peak may be explored in future studies. Also, the XRD analysis of CMC/HS revels a broad XRD band at 2θ = 21.6° which is attributed to relatively large content of organic carboxymethyl cellulose (CMC) within the polymer composites.

The FTIR technique was used to determine functional groups of (a) HS and (b) CMC/HS bio-nanocomposites in the region between 4000 and 650 cm^{-1}. FTIR results of HS and CMC/HS bio-nanocomposites are given in Fig. 3. According to the FTIR results, the characteristic peaks of HS were observed at 3442.67 cm^{-1} (–OH stretching vibration), 1477.96 cm^{-1} (C=C stretching), 1418.00 cm^{-1} (C–H asymmetric bending vibration), 1008.24 cm^{-1} (C–O stretching), and 884 cm^{-1} (C=C bending) (Karakuş et al. 2020).

Furthermore, characteristic peaks of CMC/HS bio-nanocomposites were observed at 3442.19 cm^{-1} (–OH stretching vibration), 2921.47 cm^{-1} (C–H stretching vibration), 2858.17 cm^{-1} (C–H stretching vibration), 1733.37 cm^{-1} (C=O stretching), 1584.01 cm^{-1} (C=C stretching), 1454.11 cm^{-1} (C=C stretching), 1419.39 cm^{-1} (C–H asymmetric bending vibration), 1349.28 cm^{-1} (–OH bending),

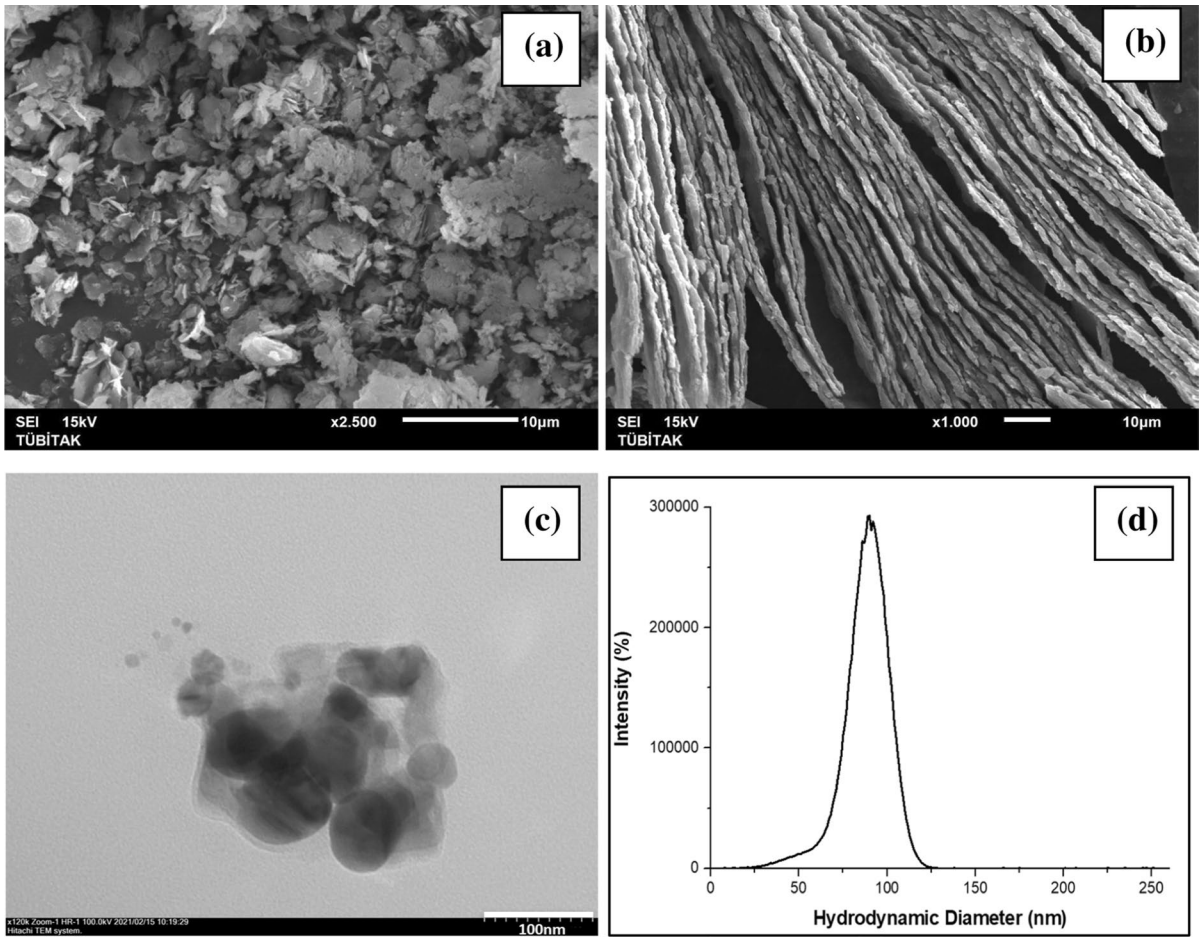

Fig. 1 SEM images of **a** HS and **b** CMC/HS, **c** TEM image and **d** hydrodynamic diameter distribution histogram of CMC/HS composite particles

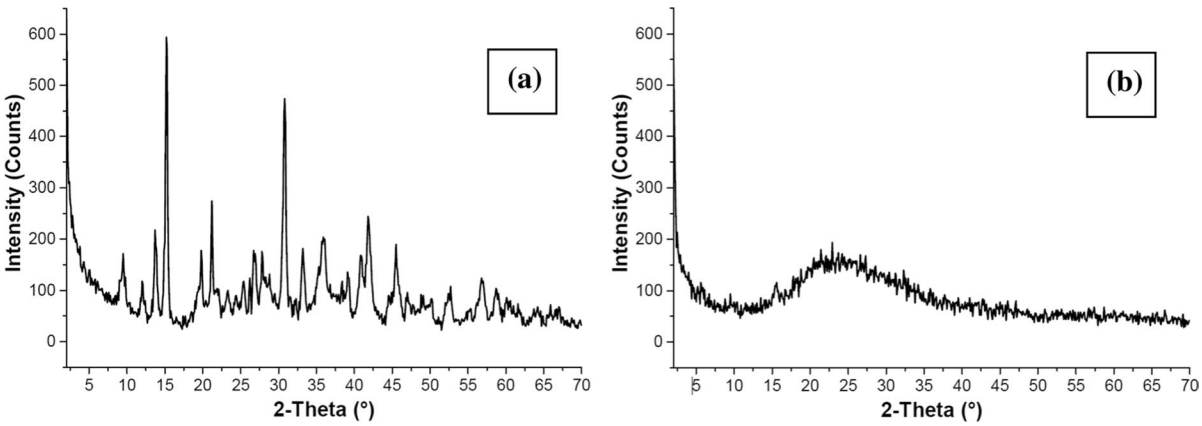

Fig. 2 XRD analysis of **a** mineral HS and **b** CMC/HS composite

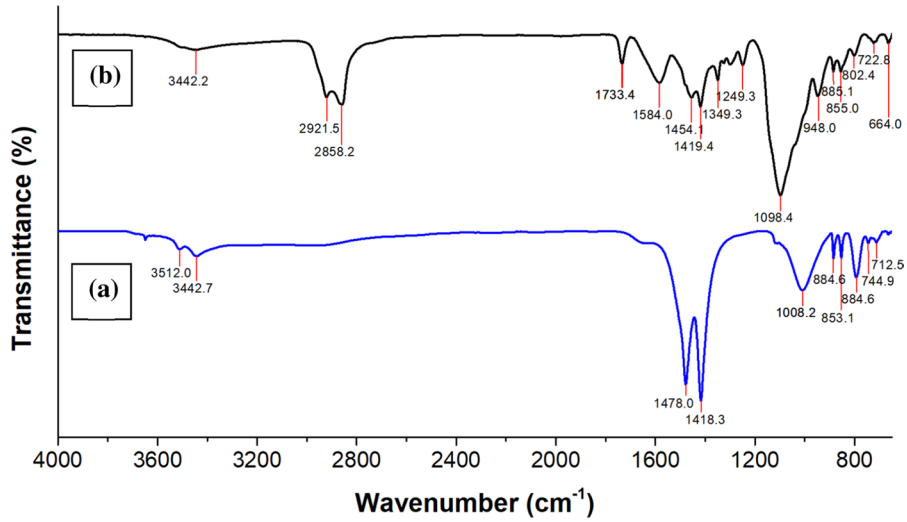

Fig. 3 FTIR results of (a) HS and (b) CMC/HS bio-nanocomposites

1299.42 cm^{-1} (C=O stretching), 1249.27 cm^{-1} (C=O stretching), 1098.42 cm^{-1} (C–O stretching), and 885 cm^{-1} (C=C bending). The interaction between HS and polymer matrix was depicted by the difference in characteristic peaks due to CH, C=O, C=C, C–O and OH functional groups. The peak intensity of the CMC/HS bio-nanocomposites was reduced at 1454.11 cm^{-1} (C=C), 1419.39 cm^{-1} (C–H). The absorbance in vibrational groups of C–H, C=O, C=C, and C–O at 2921.47 cm^{-1}, 2858.17 cm^{-1}, 1733.37 cm^{-1}, 1584.01 cm^{-1}, and 1098 cm^{-1} increased. It was shown that there is a strong interaction between the polymer matrix (CMC) and additives (HS). Furthermore, new peaks were observed at 2921.47 and 2858.17 cm^{-1} corresponding to the sp^3 hybridization peaks of alkanes with the coating of the HS with CMC in Fig. 3b. The new peak at 1733.37 cm^{-1}, especially for CMC coated with HS, could be assigned to asymmetric bands of CO_3^{-2} of HS (Camlibel et al. 2018). The characteristic peaks of HS at 1477.96 cm^{-1} and 1418.00 cm^{-1} were decreased, and a slight increase at the band intensity at 1098.42 cm^{-1} (C–O stretching) was observed. These results showed that the HS was successfully coated with CMC. Sonochemical microcavities have a significant role on the process of growth and collapse of bubbles under the ultrasonic effects (Moholkar et al. 1999). The collapse of sonochemical microcavities produces small sized nanomaterials. In this study, we used a green, low-cost, and simple sonochemical process to obtain uniform nanostructures under effect of microcavities in the solution. Furthermore, we claim that the presence of coated HS within the polymer matrix (CMC) improved the physical interaction between the HS and CMC under the ultrasonic cavitation effects with high amounts of energy.

Optimization of CMC/HS bio-nanocomposites

The interpretation of experimental viscosity data has become an important issue in material design. There is no previous research using the dilute solution methodology approach for optimization of the HS based bio-nanocomposites. Accordingly, the rheological behavior of nanofluids with detailed experimental viscosity methodology was tested to understand the morphology of the CMC/HS bio-nanocomposites and polymer–additive interactions in the aqueous solution. In summary, these rheological experiments were carried out to find out the optimum operation parameters for the novel nanostructure. The optimizations of the experimental operating parameters based on the viscosity of samples were examined for the preparation of uniform and homogenous CMC/HS bio-nanocomposites. For the experimental design of CMC/HS bio-nanocomposites, we used a simple dilute solution methodology under different experimental media. Also, we examined the rheological property of CMC/HS bio-nanocomposites to determine the effects of CMC/HS mass ratio (wt./wt.) (4:1, 3:1, and 2:1), sonication time (10–60 min), and temperature (25–45 °C) on the synthesis of the CMC/HS bio-nanocomposites.

The effects of experimental parameters such as concentration, CMC/HS mass ratio, sonication time,

and temperature on the values of [η] of CMC/HS bio-nanocomposites are shown in Figs. 4, 5 and 6. As known, the morphology, storage stability, structure and size of nanostructures are changed with the mass ratio, temperature, time, additives, and preparation method. This technique has the potential to solve design problems such as agglomeration, homogeneity, and short storage stability with a mathematical approach to the analysis of preliminary studies. However, reports in the literature on the function of rheological behavior in the morphology, structure, and miscibility of bio-nanocomposites are limited.

As known, the sonochemical effects on polymer chains in solution leads to the formation of macroradicals in the structure. The interaction between sonochemical irradiation and the sono-irradiated solution has a major role on the control of the physicochemical

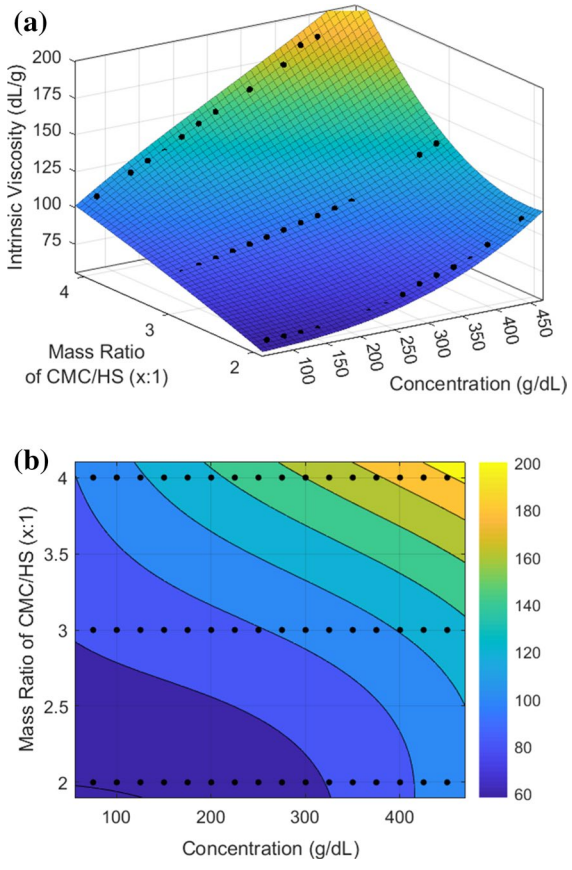

Fig. 4 The effect of the concentration and the mass ratio of CMC/HS bio-nanocomposites (wt./wt.) on [η] (sonication time is fixed at 60 min and temperature at 25 °C) illustrated in 3D coordinates (**a**) and contour plot (**b**)

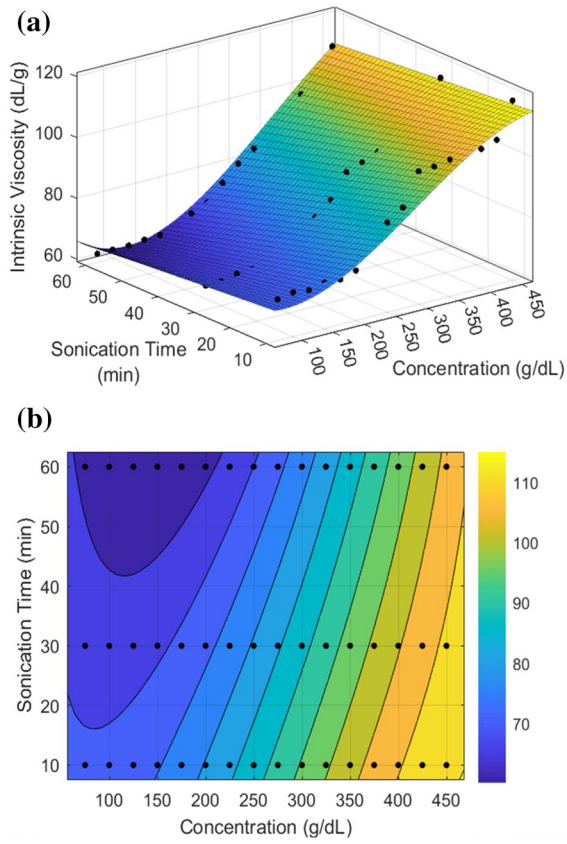

Fig. 5 The effect of the sonication time (10–60 min) on [η] of the CMC/HS bio-nanocomposite (CMC/HS ratio is fixed at 1:2 and temperature at 25 °C) illustrated in 3D coordinates (**a**) and contour plot (**b**)

parameters (surface tension and viscosity) of the nanostructure in the presence of macroradicals. However, in the literature, it was reported that there is no clear understanding of the effect of molecular weight on the rate of ultrasonic degradation (Taghizadeh and Asadpour 2009). In this study, we investigated the effect of sonication on the viscosity of the nanostructure. Additionally, we highlighted the effect of the rheological behavior and viscosity in designing the optimum nano formulation under ultrasonic cavitation (Kazemi et al. 2020; Tian et al. 2020). The results for [η] of CMC/HS bio-nanocomposites were calculated using the Huggins equation. According to experimental results, we found the optimum mass ratio for the preparation of CMC/HS bio-nanocomposites, and we calculated the results of [η] for CMC/HS bio-nanocomposites at 4:1, 3:1, and 2:1 (wt/wt) which were 75.92, 64.49, and 37.66 dl/g, respectively, with high correlation constant values (R^2)

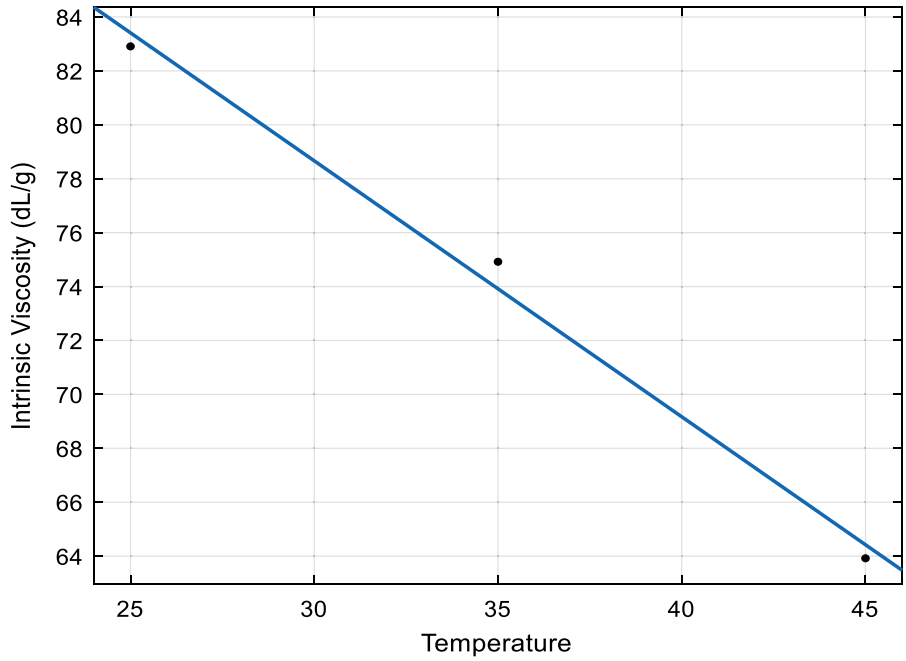

Fig. 6 The effect of the temperature (25–45 °C) on [η] of the CMC/HS bio-nanocomposite (CMC/HS ratio is 1:2 and sonication time is 60 min)

between 0.90 and 0.98 (Fig. 4). To investigate the optimization of sonication time, we calculated values of [η] for CMC/HS bio-nanocomposites. The values of [η] at different sonication times (10–60 min) were determined for CMC/HS bio-nanocomposites (wt./wt.) (2:1) at 45 °C, and they are given in Fig. 5. The values of [η] were 51.19 dl/g for 10 min, 43.96 dl/g for 30 min, and 37.66 dl/g for 60 min. We found the minimum viscosity value in the range of 63 dl/g at 45 °C (Fig. 6). Experimental results proved that the experimental optimum for variables such as sonication time, mixing ratio, and temperature are important in determining viscosity. Also, a significant mathematical correlation was revealed for the minimum viscosity based on maximum sonication time and temperature.

As shown in Fig. 4, polynomial surface fitting was utilized to obtain the intrinsic viscosity ([η]) as a function of the mass ratio of CMC/HS (wt./wt.) and concentration, as in Eq. 9. Similarly, another surface was fitted to the data of concentration, sonication time, and intrinsic viscosity as in Eq. 10 (see Fig. 5). Then, a linear regression was fitted to the intrinsic viscosity data corresponding to temperature as in Eq. 11 (see Fig. 6). The R^2 values of the regressed functions F1, F2, and F3 are 0.9929, 0.9703, and 0.9917, respectively. The coefficients of the obtained functions are given in Table 5.

$$F1(C, MR) = p00 + p10\,C + p01\,MR + p20\,C^2 + p11\,C\,MR + p02\,MR^2 + p30\,C^3 + p21\,C^2MR + p12\,CMR^2 \quad (9)$$

$$F2\left(C, t_s\right) = p00 + p10\,C + p01\,t_s + p20\,C^2 + p11\,C\,t_s + p30\,C^3 + p21\,C^2\,t_s \quad (10)$$

Table 5 Coefficients of the functions F1 and F2

F	p00	p10	p01	p20	p11	p02	p30	p21	p12
F1	−1.638	0.182	40.46	4.095e−4	−0.2101	−4.841	4.401e−7	−1.877e−4	6.122e−2
F2	75.23	−0.1043	5.328e−2	9.697e−4	−3.054e−3	N/A	−1.198e−6	5.762e−6	N/A

$$F3(T) = -0.9495\,T + 107.1 \tag{11}$$

To express the intrinsic viscosity as a single function of all operating variables, the functions F2 and F3 are normalized with respect to the fixed operating parameters (T = 25 °C and t_s = 60 min) as in Eqs. 12 and 13.

$$F2N\left(C, t_s\right) = \frac{F2\left(C, t_s\right)}{F2(C, 60)} \tag{12}$$

$$F3N(T) = \frac{F3(T)}{F3(25)} \tag{13}$$

Finally, F1 is multiplied by the normalized functions to obtain the mathematical model whose inputs are all operating variables, and the output is the intrinsic viscosity as in Eq. 14.

$$F\left(C, MR, t_s, T\right) = F3N(T) \cdot F2N\left(C, t_s\right) \cdot F1(C, MR) \tag{14}$$

Error analysis was also carried out to assess the validity of the function obtained in Eq. 14. The SSE, HYBRID, MPSD, and ARE values were evaluated by using 105 data points and presented in the Table 6. Experimental and calculated values are also compared in the correlation diagram in Fig. 7. According to the results, it can be concluded that the function obtained adequately represents the data. It was proven by characterization data that a homogeneously dispersed nanostructure was obtained under optimum conditions, and the experimental factors were found using a linear regression mathematical model. With this approach, the constructed model can successfully be used for intervals given by T = 25–45 °C, MR = 2:1–4:1, C = 75–450 g/dL, and t_s = 10–60 min.

In recent years, research has focused on improving the efficiency of nanomaterials with optimal chemical characteristics such as dispersions, viscosity, pH, etc. in biomedical applications. This study was conducted to investigate the rheological properties of prepared CMC/HS bio-nanocomposites. As a result, the mixing mass ratio of CMC/HS, temperature, sonication time, and concentration became the control and performance factors with a focus on viscosity.

Table 6 Error analysis results of the constructed model

	Constructed model (Eq. 14)
SSE	1090.99
HYBRID	11.2342
MPSD	27.5413
ARE	2.7405

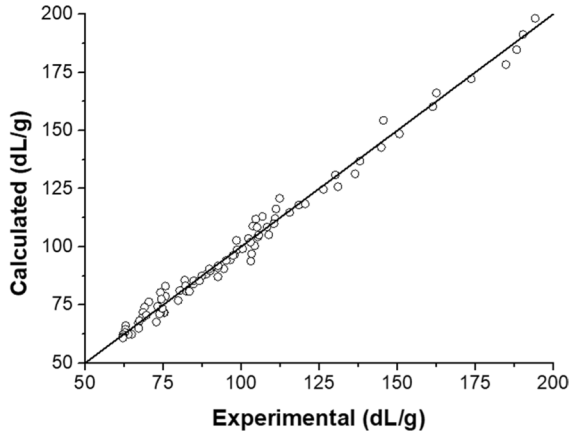

Fig. 7 Correlation diagram of calculated and experimental intrinsic viscosity values

Challenge test of CMC/HS bio-nanocomposites

Recently, new advanced nanomaterials with high antimicrobial and antifungal activities have become vital solutions for pathogenic microorganism problems. For this reason, they have a key function to prevent the spread of these pathogenic problems such as Coronavirus disease 2019 (COVID-19), Ebola, and influenza A (H1N1) disease by using effective and fast nanotechnological solutions using nanoscale materials. With this approach, we developed novel and green CMC/HS bio-nanocomposites and examined the biological activities such as antimicrobial and antifungal properties of the bio-nanocomposites to evaluate them against pathogenic microorganisms such as *S. aureus, P. aeruginosa, E. coli, C. albicans,* and *A. brasiliensis*. These pathogenic microorganisms transmit diseases directly/indirectly from person to person and from animal to person (Tewari et al. 2021).

The total aerobic mesophilic microorganism (lSO 21149) and mold—yeast (lSO 16212) guidelines were used for the antimicrobial and antifungal properties

of the prepared CMC/HS bio-nanocomposites. The preservative results of CMC/HS bio-nanocomposites against pathogenic microorganisms (*S. aureus, P. aeruginosa, E. coli, C. albicans,* and *A. brasiliensis*) are given in Fig. 8a–e. In the literature, the antimicrobial mechanism of nanostructures is generally explained as depending on different approaches such as the generation of reactive oxygen species (ROS), penetration of the bacterial cell membrane, metal ion release, and mechanical damage to the cell membrane (Arakha et al. 2015). Especially, the unique small nanosize of the nanostructure has a major role on the penetration and mechanical damage to the cell membrane of pathogenic microorganisms. The novel

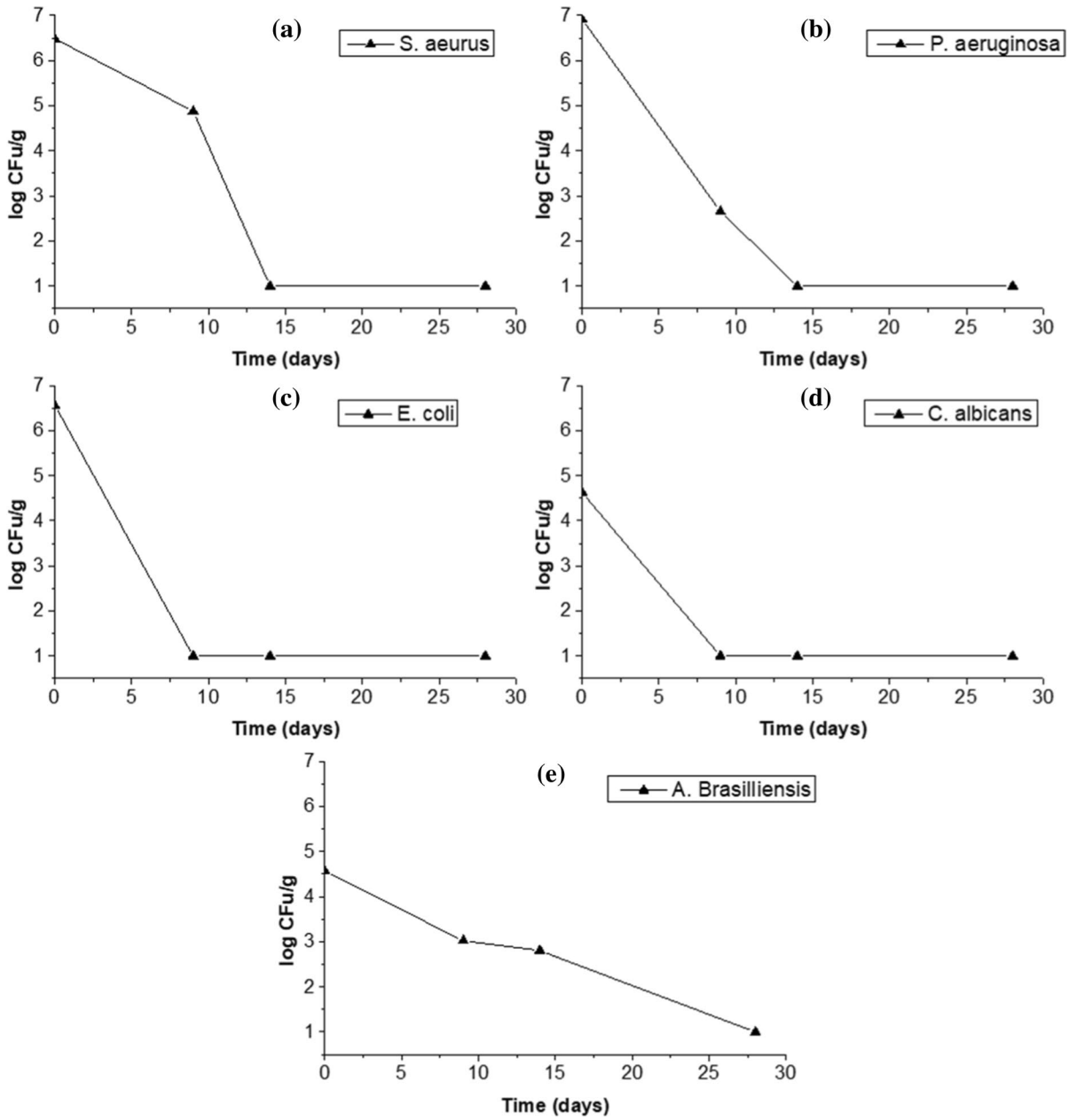

Fig. 8 The preservative results of the prepared CMC/HS bio-nanocomposites against pathogenic microorganisms **a** *S. aureus*, **b** *P. aeruginosa*, **c** *E. coli*, **d** *C. albicans*, and **e** *A. brasiliensis*

aspect of this research included the first-time use of the prepared CMC/HS with a mean particle size less than 100 nm in antimicrobial studies. According to the experimental results, we assumed that the small size of CMC/HS had a function on the damage to the cell membrane of pathogenic microorganisms and leakage of intracellular components from bacterial cells medium. It was observed that the criterion A was satisfied for the prepared CMC/HS bio-nanocomposites. To our knowledge, this study is the first report on antimicrobial and antifungal properties of the prepared HS based bio-nanocomposites against *S. aureus, P. aeruginosa, E. coli, C. albicans,* and *A. brasiliensis* for use in cosmetic preparations.

In the literature, several reports have focused on green additive-based nanocomposites with high antimicrobial and antifungal against pathogenic microorganisms. The experimental result of the novel nanostructure showed that it had high antimicrobial and antifungal activities, and these results were appreciable from the comparison with previous studies (Table 7).

In vitro cytotoxicity evaluation of CMC/HS bio-nanocomposites

The cytotoxicity of CMC, HS, and CMC/HS bio-nanocomposites was investigated on L929 cells by the MTT assay. The results showed that CMC, HS, and synthesized CMC/HS bio-nanocomposites have no cytotoxic effects on L929 cells after 24 h incubation. As shown in Fig. 9, no significant difference was observed among CMC, HS, and CMC/HS bio-nanocomposites. Based on MTT results, all samples exhibited high cell viability and healthy growth. CMC is reported to be physiologically nontoxic and is compatible with mucous membranes, bone, and skin (Basu et al. 2018; Ahmad 2021; Rahman et al. 2021). Therefore, the use of CMC has been widely established in pharmaceutical, drug and protein delivery, and wound healing applications (Priya et al. 2021). Also, the use of CMC as a feed additive is considered safe for the environment and for the consumers (Bampidis et al. 2020). Consequently, we propose that the synthesized CMC/HS bio-nanocomposites are cytocompatible and non-toxic, which is consistent with our results. Thus, CMC/HS bio-nanocomposites could be suitable for as alternative green preservative nano-additives against pathogenic microorganisms.

Results were expressed as percentage of control (untreated cells) cell viability. Each bar represents a mean ± SE (n = 3), $p < 0.05$. Morphology of L929 cells was observed with an inverted microscope under 400× magnification.

Table 7 The comparison of biological activities of the various green bio-nanostructures

Sample	Morphology	Microorganisms	References
TiO_2/cellulose nanocomposites	Spherical, 100 nm	*E. coli*	Zong et al. (2021)
Kiwi peel phenolic extracts bio-reduced silver nanoparticles	Dendritic structure, 124 nm	*E. coli* and *S. aureus*	Sun et al. (2021)
Plant and lichen extracts-based Ag-MgO nanocomposites	Worm like, berries-like, needle-like, and semi-spherical 69–104 nm	*E. coli, P. aeruginosa,* and *S. aurea*	Alavi and Karimi (2020)
Selenium nanoparticles	Polygonal and 83 nm	*E. coli, Salmonella typhimurium,* and *Bacillus cereus*	Ndwandwe et al. (2021)
CMC stabilized nano silver	Spherical, 5–15 nm	*Human bacterial pathogens*	Prema et al. (2017)
Nanocellulose/CMC and nano-chitosan/CMC composite films	–	*E. coli* and *S. aureus*	Jannatyha et al. (2020)
Polyvinyl alcohol-CMC/ZnO nanocomposite	Fiber, 214–239 nm	*E. coli* and *S. aureus*	Darbasizadeh et al. (2019)
CMC supported gold nanoparticles	Spherical, 12–20 nm	*E. coli, P. aeruginosa, S. aureus* and *B. subtilis*	Fouda et al. (2020)
CMC/HS bio-nanocomposites	2D layers, 100 nm	*S. aureus, P. aeruginosa, E. coli, C. albicans,* and *A. brasiliensis*	This study

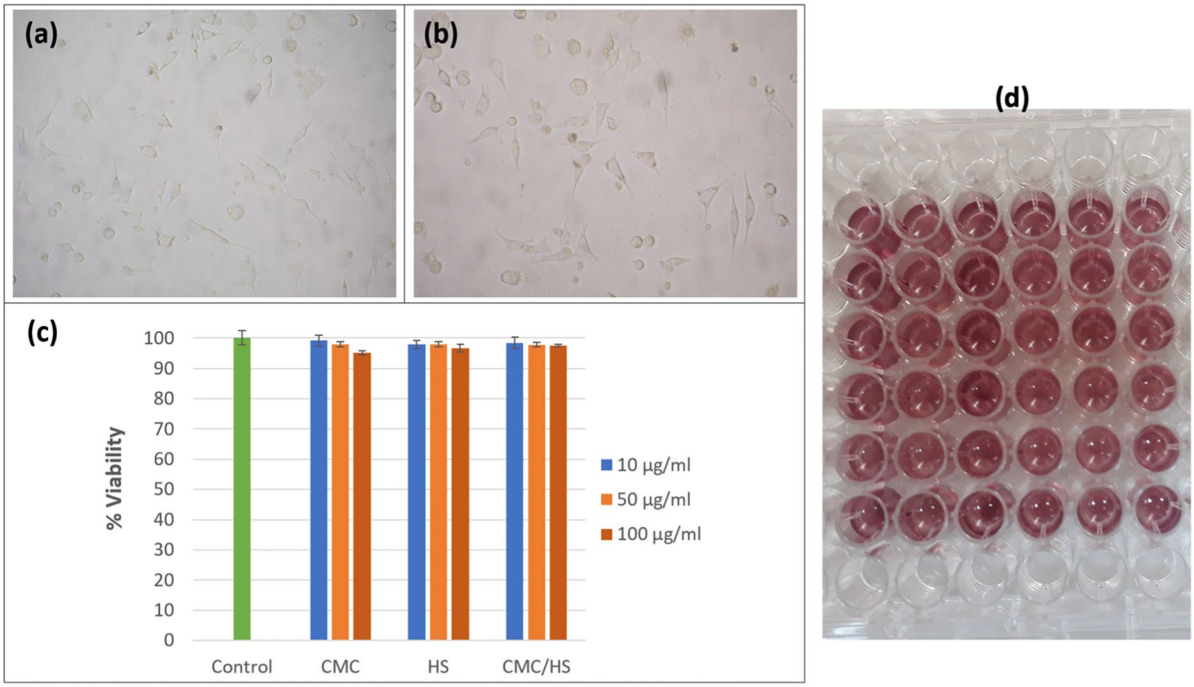

Fig. 9 **a** Control (untreated cells), **b** cells treated with 100 µg/ml of CMC/HS bio-nanocomposites, **c** cell survival (MTT assay) of L929 cells exposed to the CMC, HS, and CMC/HS bio-nanocomposites for 24 h and **d** the image of MTT assay

Conclusion

In this study, the novel bio-nanocomposite containing CMC/HS was prepared using a green and simple sonochemical method. The characterization results showed that the prepared bio-nanocomposites have a homogeneous 2D nanostructure, an XRD crystallite size of 16.90 nm, and a large surface area (180.66 m^2/g). Furthermore, the relationships between the intrinsic viscosity of the bio-nanocomposite and operating variables were examined, and a mathematical model was constructed to investigate the optimum experimental conditions. According to our results, the minimum intrinsic viscosity can be obtained in the shortest amount of sonication time at a concentration of 100–150 g/dL. The lower mass fraction of CMC/HS (2:1) and higher temperatures (45 °C) resulted lower intrinsic viscosity. However, lower intrinsic viscosity values may also be achieved by increasing the sonication time instead of increasing the temperature. Finally, the antimicrobial and antifungal effects of CMC/HS bio-nanocomposites were examined against pathogenic microorganisms such as *S. aureus, P. aeruginosa, E. coli, C. albicans,* and *A. brasiliensis*. Also, the cytotoxicity of CMC/HS bio-nanocomposites was evaluated on L929 cells. MTT assay results showed that the nanostructure had non-toxic and cytocompatibility properties. Consequently, we proved that the novel green preservative CMC/HS bio-nanocomposites had excellent antibacterial and antifungal activities corresponding to the criteria A.

Acknowledgments The authors kindly acknowledge the East Anatolia High Technology Application and Research Center (DAYTAM) at Ataturk University for providing characterization.

Funding The authors have not disclosed any funding.

Declarations

Conflict of interest The authors declare no conflict of interest.

References

Abduraimova A, Molkenova A, Duisembekova A et al (2021) Cetyltrimethylammonium bromide (CTAB)-loaded

SiO_2–Ag mesoporous nanocomposite as an efficient antibacterial agent. Nanomaterials 11:477
Ahmad H (2021) Celluloses as support materials for antibacterial agents: a review. Cellulose 28(5):2715–2761
Ahmed F, Faisal SM, Ahmed A, Husain Q (2020) Beta galactosidase mediated bio-enzymatically synthesized nanogold with aggrandized cytotoxic potential against pathogenic bacteria and cancer cells. J Photochem Photobiol B Biol 209:111923
Akao M, Iwai S, IUCr (1977) The hydrogen bonding of hydromagnesite. Acta Crystallogr B 33:1273–1275
Alafeef M, Moitra P, Pan D (2020) Nano-enabled sensing approaches for pathogenic bacterial detection. Biosens Bioelectron 165:112276
Alavi M, Karimi N (2020) Hemoglobin self-assembly and antibacterial activities of bio-modified Ag-MgO nanocomposites by different concentrations of Artemisia haussknechtii and Protoparmeliopsis muralis extracts. Int J Biol Macromol 152:1174–1185
Amina M, al Musayeib NM, Al-Hamoud GA et al (2021) Prospective of biosynthesized L.satiVum oil/PEG/Ag-MgO bionanocomposite film for its antibacterial and anticancer potential. Saudi J Biol Sci 28:5971–5985
Arakha M, Saleem M, Mallick BC, Jha S (2015) The effects of interfacial potential on antimicrobial propensity of ZnO nanoparticle. Sci Rep 5(1):1–10
Awad ME, López-Galindo A, Medarević D et al (2021) Enhanced antimicrobial activity and physicochemical stability of rapid pyro-fabricated silver-kaolinite nanocomposite. Int J Pharm 598:120372
Bampidis V, Azimonti G, de L Bastos M, et al (2020) Safety and efficacy of sodium carboxymethyl cellulose for all animal species. EFSA J 18:e06211
Baptista PV, McCusker MP, Carvalho A et al (2018) Nano-strategies to fight multidrug resistant bacteria—"A Battle of the Titans." Front Microbiol 9:1441
Barman M, Mahmood S, Augustine R et al (2020) Natural halloysite nanotubes/chitosan based bio-nanocomposite for delivering norfloxacin, an anti-microbial agent in sustained release manner. Int J Biol Macromol 162:1849–1861
Basu P, Narendrakumar U, Arunachalam R et al (2018) Characterization and evaluation of carboxymethyl cellulose-based films for healing of full-thickness wounds in normal and diabetic rats. ACS Omega 3:12622–12632
Braithwaite CJR, Zedef V (1994) Living hydromagnesite stromatolites from Turkey. Sed Geol 92:1–5
Camlibel NO, Avinc O, Arik B et al (2018) The effects of huntite–hydromagnesite inclusion in acrylate-based polymer paste coating process on some textile functional performance properties of cotton fabric. Cellulose 26(2):1367–1381
Connolly M, Zhang Y, Brown DM et al (2019) Novel polylactic acid (PLA)-organoclay nanocomposite bio-packaging for the cosmetic industry; migration studies and in vitro assessment of the dermal toxicity of migration extracts. Polym Degrad Stab 168:108938
Darbasizadeh B, Fatahi Y, Feyzi-barnaji B et al (2019) Crosslinked-polyvinyl alcohol-carboxymethyl cellulose/ZnO nanocomposite fibrous mats containing erythromycin (PVA-CMC/ZnO-EM): fabrication, characterization and in-vitro release and anti-bacterial properties. Int J Biol Macromol 141:1137–1146
Fouda MMG, Ajarem JS, Maodaa SN et al (2020) Carboxymethyl cellulose supported green synthetic features of gold nanoparticles: antioxidant, cell viability, and antibacterial effectiveness. Synth Met 269:116553
Ghosh S, Singh BP, Webster TJ (2021) Nanoparticle-impregnated biopolymers as novel antimicrobial nanofilms. In: Biopolymer-based nano films, pp 269–309
Guo Y, Zhao C, Yan C, Cui L (2021) Construction of cellulose/carboxymethyl chitosan hydrogels for potential wound dressing application. Cellulose 28(15):10013–10023
Hassanen EI, Ragab E (2020) In vivo and in vitro assessments of the antibacterial potential of chitosan-silver nanocomposite against methicillin-resistant *Staphylococcus aureus*–induced infection in rats. Biol Trace Elem Res 199(1):244–257
Jannatyha N, Shojaee-Aliabadi S, Moslehishad M, Moradi E (2020) Comparing mechanical, barrier and antimicrobial properties of nanocellulose/CMC and nanochitosan/CMC composite films. Int J Biol Macromol 164:2323–2328
Karakus S, Ilgar M, Kahyaoglu IM, Kilislioglu A (2019) Influence of ultrasound irradiation on the intrinsic viscosity of guar gum–PEG/rosin glycerol ester nanoparticles. Int J Biol Macromol 141:1118–1127
Karakuş S, Taşaltın N, Taşaltın C, Kilislioğlu A (2020) Comparative study on ultrasonic assisted adsorption of Basic Blue 3, Basic Yellow 28 and Acid Red 336 dyes onto hydromagnesite stromatolite: kinetic, isotherm and error analysis. Surf Interfaces 20:100528
Karakuş S, Albayrak İ, Üllen NB et al (2021) Preparation, characterization and evaluation of a novel CMC/Chitosan-α-Fe2O3 nanoparticles-coated 17–4 PH stainless-steel foam. Polym Bull 2021:1–19
Kasirajan L, Maupin-Furlow JA (2021) Halophilic archaea and their potential to generate renewable fuels and chemicals. Biotechnol Bioeng 118:1066–1090
Kazemi I, Sefid M, Afrand M (2020) A novel comparative experimental study on rheological behavior of mono & hybrid nanofluids concerned graphene and silica nanopowders: characterization, stability and viscosity measurements. Powder Technol 366:216–229
Kibasomba PM, Dhlamini S, Maaza M et al (2018) Strain and grain size of TiO2 nanoparticles from TEM, Raman spectroscopy and XRD: the revisiting of the Williamson-Hall plot method. Results Phys 9:628–635
Kouser S, Sheik S, Prabhu A et al (2021) Effects of reinforcement of sodium alginate functionalized halloysite clay nanotubes on thermo-mechanical properties and biocompatibility of poly(vinyl alcohol) nanocomposites. J Mech Behav Biomed Mater 118:104441
Kumaravel V, Nair KM, Mathew S et al (2021) Antimicrobial TiO2 nanocomposite coatings for surfaces, dental and orthopaedic implants. Chem Eng J 416:129071
Moghadam A, Salmani Mobarakeh M, Safaei M, Kariminia S (2021) Synthesis and characterization of novel bio-nanocomposite of polyvinyl alcohol-Arabic gum-magnesium oxide via direct blending method. Carbohydr Polym 260:117802

Moholkar VS, Senthil Kumar P, Pandit AB (1999) Hydrodynamic cavitation for sonochemical effects. Ultrason Sonochem 6:53–65

Murali S, Kumar S, Koh J et al (2019) Bio-based chitosan/gelatin/Ag@ZnO bionanocomposites: synthesis and mechanical and antibacterial properties. Cellulose 26(9):5347–5361

Navik R, Thirugnanasampanthan L, Venkatesan H et al (2017) Synthesis and application of magnesium peroxide on cotton fabric for antibacterial properties. Cellulose 24(8):3573–3587

Ndwandwe BK, Malinga SP, Kayitesi E, Dlamini BC (2021) Solvothermal synthesis of selenium nanoparticles with polygonal-like nanostructure and antibacterial potential. Mater Lett 304:130619

Nguyen KT, Mai DXN, Doan UTT et al (2021) The chitosan/ZnO bio-nanocomposites with selective antibacterial efficiency. J Mater Res 36(2):508–517

Nishida K, Kaji K, Kanaya T, Fanjat N (2002) Determination of intrinsic viscosity of polyelectrolyte solutions. Polymer 43:1295–1300

Othman SH, Othman NFL, Shapi'i RA et al (2021) Corn starch, chitosan nanoparticles, thymol bio-nanocomposite films for potential food packaging applications. Polymers 13:390

Prema P, Thangapandiyan S, Immanuel G (2017) CMC stabilized nano silver synthesis, characterization and its antibacterial and synergistic effect with broad spectrum antibiotics. Carbohydr Polym 158:141–148

Priya G, Madhan B, Narendrakumar U et al (2021) In vitro and in vivo evaluation of carboxymethyl cellulose scaffolds for bone tissue engineering applications. ACS Omega 6:1246–1253

Rahman MS, Hasan MS, Nitai AS et al (2021) Recent developments of carboxymethyl cellulose. Polymers 13:1345

Rao KM, Suneetha M, Park GT et al (2020) Hemostatic, biocompatible, and antibacterial non-animal fungal mushroom-based carboxymethyl chitosan-ZnO nanocomposite for wound-healing applications. Int J Biol Macromol 155:71–80

Saadat S, Pandey G, Tharmavaram M et al (2020) Nano-interfacial decoration of Halloysite Nanotubes for the development of antimicrobial nanocomposites. Adv Colloid Interface Sci 275:102063

Sahoo M, Vishwakarma S, Panigrahi C, Kumar J (2021) Nanotechnology: current applications and future scope in food. Food Front 2:3–22

Scaffaro R, Botta L, Lopresti F et al (2017) Polysaccharide nanocrystals as fillers for PLA based nanocomposites. Cellulose 24:447–478

Shahvalizadeh R, Ahmadi R, Davandeh I et al (2021) Antimicrobial bio-nanocomposite films based on gelatin, tragacanth, and zinc oxide nanoparticles—microstructural, mechanical, thermo-physical, and barrier properties. Food Chem 354:129492

Sharma R, Jafari SM, Sharma S (2020) Antimicrobial bionanocomposites and their potential applications in food packaging. Food Control 112:107086

Sun X, Zhang H, Wang J et al (2021) Sodium alginate-based nanocomposite films with strong antioxidant and antibacterial properties enhanced by polyphenol-rich kiwi peel extracts bio-reduced silver nanoparticles. Food Packag Shelf Life 29:100741

Taghizadeh MT, Asadpour T (2009) Effect of molecular weight on the ultrasonic degradation of poly(vinyl-pyrrolidone). Ultrason Sonochem 16:280–286

Tewari A, Jain B, Brar B, et al (2021) Biosensors: modern tools for disease diagnosis and animal health monitoring. In: Biosensors in agriculture: recent trends and future perspectives, p 387

Tian Z, Rostami S, Taherialekouhi R et al (2020) Prediction of rheological behavior of a new hybrid nanofluid consists of copper oxide and multi wall carbon nanotubes suspended in a mixture of water and ethylene glycol using curve-fitting on experimental data. Phys A Stat Mech Appl 549:124101

Tsirigotis-Maniecka M (2020) Alginate-, carboxymethyl cellulose-, and κ-carrageenan-based microparticles as storage vehicles for cranberry extract. Molecules 25:3998

Wang Y, Cen C, Chen J, Fu L (2020) MgO/carboxymethyl chitosan nanocomposite improves thermal stability, waterproof and antibacterial performance for food packaging. Carbohydr Polym 236:116078

Wang Y, Yi S, Lu R et al (2021) Preparation, characterization, and 3D printing verification of chitosan/halloysite nanotubes/tea polyphenol nanocomposite films. Int J Biol Macromol 166:32–44

Yunusov KE, Sarymsakov AA, Jalilov JZO, Atakhanov AAO (2021) Physicochemical properties and antimicrobial activity of nanocomposite films based on carboxymethylcellulose and silver nanoparticles. Polym Adv Technol 32:1822–1830

Zhang YY, Xu QB, Fu FY (2016) Liu XD (2016) Durable antimicrobial cotton textiles modified with inorganic nanoparticles. Cellulose 23(5):2791–2808

Zong E, Wang C, Yang J et al (2021) Preparation of TiO2/cellulose nanocomposites as antibacterial bio-adsorbents for effective phosphate removal from aqueous medium. Int J Biol Macromol 182:434–444